Superconductivity and magnetism in the Heusler alloys $M\mathrm{Pd}_2\mathrm{Pb}$ (M=rare earth, Th, and U)

C. L. Seaman,* N. R. Dilley, M. C. de Andrade, J. Herrmann, M. B. Maple, and Z. Fisk†
Department of Physics and Institute for Pure and Applied Physical Sciences, University of California, San Diego, La Jolla, California 92093
(Received 27 September 1995)

We report on an investigation of superconductivity and magnetism in the series of compounds $M\mathrm{Pd}_2\mathrm{Pb}$ (M=rare earth, Th, U) through measurements of electrical resistivity, magnetic susceptibility, specific heat, and lattice parameters. Both single crystals and polycrystalline samples were studied. The compound $\mathrm{UPd}_2\mathrm{Pb}$ was examined for possible heavy-fermion behavior, and found to exhibit antiferromagnetic order below T=35 K.

INTRODUCTION

Several Heusler alloys (cubic $L2_1$ structure) with the general chemical formula RT_2X have been found to exhibit superconductivity, including YPd_2X (X=Sn, Pb, In, and Sb),[1] $\mathrm{YAu}_2\mathrm{Sn}$,[2] and $R\mathrm{Pd}_2\mathrm{Sn}$ (R=Sc, Y, Tm, Yb, and Lu),[1,3] with critical temperatures as high as 4.76 K. Moreover, superconductivity and antiferromagnetism coexist in the compound $\mathrm{YbPd}_2\mathrm{Sn}$. Higher T_c values were generally found for compounds with larger lattice parameters, with $\mathrm{YPd}_2\mathrm{Pb}$ yielding the highest reported value of 4.76 K.[1] For $R\mathrm{Pd}_2\mathrm{Pb}$ samples, we also expected the effects of magnetic pair breaking by the magnetic R ions to be minimized because of the large lattice parameters, which could give rise to interesting effects due to the interaction and competition between superconductivity and magnetism. We report on an investigation of superconductivity and magnetism in the series of compounds $M\mathrm{Pd}_2\mathrm{Pb}$ (M=rare earth R, Th, and U), primarily through measurements of electrical resistivity and magnetic susceptibility. Both polycrystalline samples and single crystals were studied. We find that the magnetic rare-earth ions order antiferromagnetically at low temperatures with the lowest Néel temperature T_N values among $R\mathrm{Pd}_2X$ compounds. Bulk superconductivity is found for R=Sc, Y, Tm, Yb, and Lu, but with lower T_c values than expected, probably associated with sample quality. Motivated by heavy-fermion behavior previously observed in $\mathrm{UPd}_2\mathrm{Sn}$,[4] the compound $\mathrm{UPd}_2\mathrm{Pb}$ was examined for possible heavy-fermion behavior, and found to exhibit antiferromagnetic order below T=35 K, inferred from a sharp cusp observed in the magnetic susceptibility. The large value of the linear coefficient of the specific heat $\gamma\approx$100 mJ/mol K^2, determined from data measured below 35 K, along with the temperature dependence of the electrical resistivity, suggest that this may be an antiferromagnetic low effective mass heavy-fermion compound.

EXPERIMENTAL DETAILS

Single crystals and polycrystalline samples of $M\mathrm{Pd}_2\mathrm{Pb}$ were fabricated by flux growth and by melting in sealed Ta tubes, respectively. Powder x-ray-diffraction measurements were subsequently made using a Rigaku rotating-anode diffractometer utilizing Cu $K\alpha$ radiation. Electrical-resistivity measurements were made on the polycrystalline samples from 1 to 300 K in a ^{4}He cryostat using a self-balancing, four-wire ac resistance bridge operating at 16 Hz, with typical excitation current densities of $\sim$100 μA/cm^2. Platinum electrical leads (50 μm diameter) were attached with silver epoxy. Static magnetic-susceptibility measurements were performed on single crystals using a Quantum Design superconducting quantum interference device (SQUID) magnetometer from 1.8 to 300 K in magnetic fields up to 7 T. Low-temperature ($0.2\leqslant T\leqslant 6$ K) ac magnetic-susceptibility measurements were performed in a ^{3}He/^{4}He dilution refrigerator. Specific-heat measurements were made on a polycrystalline sample of $\mathrm{UPd}_2\mathrm{Pb}$ from 0.5 to 20 K using a semiadiabatic heat-pulse calorimeter utilizing a ^{3}He cryostat.

SAMPLE PREPARATION

Single crystals of $M\mathrm{Pd}_2\mathrm{Pb}$ were successfully grown in Pb flux for M=Sc, Y, Gd, Tb, Dy, Ho, Er, Tm, and Lu. Attempts to grow crystals with M=Yb and U were unsuccessful, even though polycrystalline samples could be prepared by arc melting. In addition, attempts to grow crystals consisting of the lighter rare-earth ions M=Ce, Pr, Nd, Sm, and Eu were unsuccessful, consistent with our inability to make polycrystalline samples, most likely due to the large size of the trivalent ions. The crystals were prepared in the following way.

Stoichiometric amounts of 99.9% pure M and 99.99% pure Pd were placed in an alumina crucible with 99.999% pure Pb, which comprised 90 mol % of the mixture. Quartz wool was then placed inside the crucible, which was then sealed in a quartz tube and backfilled with 150 torr ultrahigh-purity (UHP) Ar. The sample was heated to 1200 °C, then slowly cooled (10 °C/h), allowing single crystals to nucleate. In our case, Pb from the flux was incorporated into the crystal structure. The sample was removed from the furnace at 800 °C and centrifuged immediately so that the molten flux spun through the quartz wool, leaving the crystals in the crucible. To etch away any remaining free Pb, the crystals were placed in a 1:1 solution of H_2O_2 (30%): glacial acetic acid for no more than 5 min. The crystals formed as cubes or clusters of cubes which appeared to grow in the (111) direction. Of these, crystals with M=Gd and Sc formed the largest- ($\sim$1 mm on a side) and smallest-sized cubes, respectively.

Subsequent x-ray powder diffraction of powdered crystals verified the single-phase $L2_1$ cubic Heusler structure for R=Lu, Tm, Er, Ho, Dy, Tb, Gd, Y, and Sc. No impurity

peaks, including those of free Pb, were evident in the x-ray patterns. The intensity of the background noise level was only ~0.1% of the most intense peak corresponding to the (220) direction. The flux growths with Gd and Eu contained long, needle-shaped crystals (~5 mm length), but they exhibited multiple x-ray peaks which did not belong to the Heusler structure. The Gd flux growths also contained the cube-shaped crystals with the Heusler structure. $ThPd_2Pb$ formed, though it contained several impurity phases, one of which was identified as ThPb. Attempts to grow single crystals of R=Yb, Eu, Sm, Nd, Pr, Ce, and U were unsuccessful.

Polycrystalline samples were fabricated by melting in Ta tubes as follows. Stoichiometric amounts of each element were sealed in a 1-cm-diameter Ta tube, with 1 atm UHP Ar. The tube was then sealed in a quartz tube backfilled to 150 torr UHP Ar, heated to 1300 °C for 1 h, and subsequently quenched by placing the 1300 °C tube in water at room temperature. Samples with the Heusler structure were made for R=Sc, Y, Tb, Dy, Ho, Tm, Yb, and U. X-ray powder-diffraction data revealed trace amounts of elemental Pb (a superconductor with T_c=7.2 K) in all samples, Pb_2Pd (a superconductor with T_c=3.0 K) for R=Y, Dy, Ho, and Tm, and RPd_3 (not superconducting) for R=Yb. This method was not successful for R=Ce, Eu, Gd, Lu, or Th, although a minority Heusler phase was still discernible for Lu. The R=Er sample was made by arc melting with excess Pb to compensate for loss due to its high vapor pressure. None of the samples were subsequently annealed.

It is interesting to note that the related compounds RPd_2Sn, with R=Tb and Dy, exhibit structural transformations at ~250 and 50 K, respectively, which lowers the crystal symmetries.[5] The transformations were not evident from magnetic susceptibility, and we cannot rule out similar transformations occurring in our RPd_2Pb samples.

RESULTS AND DISCUSSION

RPd_2Pb (R=rare earth: Sc,Y,Gd,Tb,Dy,Ho,Er,Tm,Yb,Lu)

Electrical resistivity

Shown in Fig. 1 is the temperature dependence of the normal-state electrical resistivity $\rho(T)$, normalized to its room-temperature value, of RPd_2Pb compounds in which the $4f$ electron shell of the R ions is (a) empty or filled and (b) partially filled. Except for R=Gd, for which a single crystal was used, polycrystalline samples were measured because of the difficulty of attaching electrical leads to the extremely small crystals. All samples exhibit metallic behavior with positive temperature coefficient of resistance at all temperatures below 295 K. The data display downward curvature except at the lowest temperatures where phonon scattering freezes out and the data eventually saturate towards the zero-temperature value due to scattering by defects and impurities. Although the degree of curvature varies among the RPd_2Pb samples, it does not appear to depend in a systematic way on the R ion. In particular, temperature-dependent magnetic scattering due to splitting of the ground-state multiplet by the crystalline electric field (CEF) is not obvious. The resistance ratio RR=ρ(295 K)/ρ(0 K) also varies a lot among samples, attesting to varying amounts of impurity scattering.

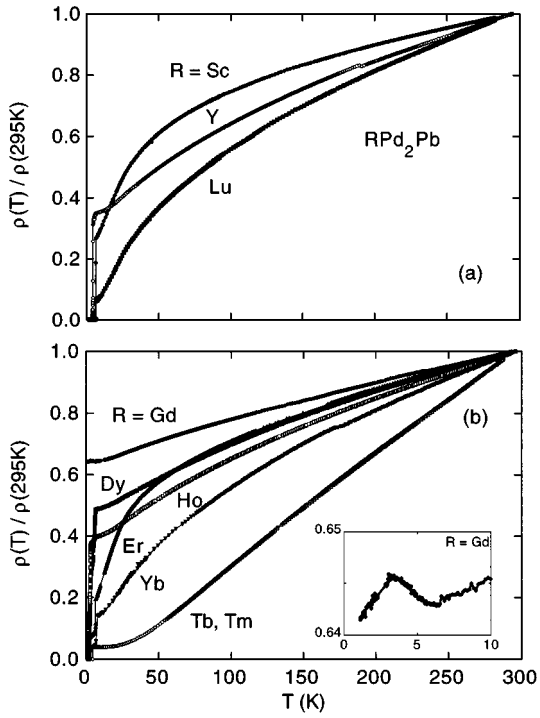

FIG. 1. Normal-state electrical resistivity normalized to its room-temperature value, $\rho(T)/\rho(295\ \mathrm{K})$, vs temperature T for RPd_2Pb polycrystalline samples in which the $4f$ electron shell of the R ion is (a) empty or filled and (b) partially filled. Data for R=Gd are for a single crystal. Resistivity drops at $T\approx7$ K are due to Pb inclusions.

Qualitatively speaking, those samples with the largest-moment R ions, namely, R=Gd, Ho, and Dy, exhibit the smallest RR's.

All of the polycrystalline samples have elemental Pb impurities, which causes $\rho(T)$ to drop below $T\approx7$ K owing to the superconductivity of Pb. For those samples in which $\rho(T)$ does not drop to zero by then, an additional drop is observed below $T\approx3$ K due to the presence of a Pb_2Pd impurity phase, which is superconducting with T_c=3.0 K.[6] No such resistive drops are observed for the relatively impurity-free single-crystal specimen of $GdPd_2Pb$, allowing a small anomaly in $\rho(T)$, shown in the inset of Fig. 1(b), to be observed near T=4.5 K. This anomaly is due to antiferromagnetic ordering of the Gd moments, as inferred from the magnetic susceptibility discussed below.

Magnetic susceptibility

Shown in Fig. 2 is the inverse magnetic susceptibility χ^{-1} as a function of temperature T for the RPd_2Pb compounds with magnetic rare-earth ions R. The $\chi(T)$ data were acquired for many clusters of single crystals with random orientations with respect to the magnetic-field direction, except for R=Er for which a polycrystalline sample was measured. Over a wide temperature range ($10\leq T\leq300$ K), the data for all of these samples are well described by the Curie-Weiss law $\chi(T)=N\mu_{\mathrm{eff}}^2/3k_B(T-\theta_{\mathrm{CW}})$, where N is the number of rare-earth ions, μ_{eff} is the effective magnetic moment, and θ_{CW} is the Curie-Weiss temperature. The solid lines in Fig. 2 represent least-squares linear fits of the data, which yield

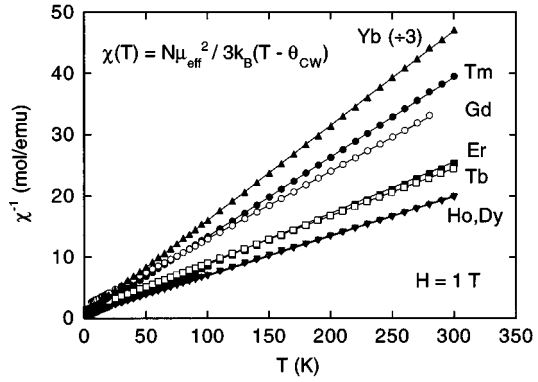

FIG. 2. Inverse magnetic susceptibility χ^{-1} vs temperature T for $R\mathrm{Pd}_2\mathrm{Pb}$ single crystals, where R has a partially filled $4f$ electron shell. The measurements were made in a field of 1 T for $1.8 \leqslant T \leqslant 300$ K.

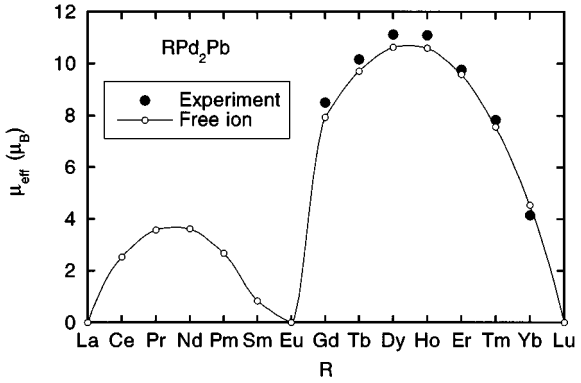

FIG. 3. Effective magnetic moments μ_{eff} of the rare-earth ions R in $R\mathrm{Pd}_2\mathrm{Pb}$ (solid circles), derived from Curie-Weiss fits to the magnetic susceptibility, compared to the theoretical free-ion values (open circles).

values for μ_{eff} and θ_{CW} listed in Table I. The values of μ_{eff} are close to the theoretical Hund's rules ground-state values for free trivalent rare-earth ions as illustrated in Fig. 3 and do not deviate much from the Curie-Weiss fits above the antiferromagnetic ordering temperatures, suggesting that the CEF energy level splittings Δ_{CEF} of the Hund's rules ground-state multiplets are small ($\Delta_{\mathrm{CEF}} < 10$ K≈ 1 meV) in these compounds.

The Curie-Weiss temperatures θ_{CW} are all negative, indicative of antiferromagnetic (AFM) exchange interactions. These interactions give rise to AFM order at low temperatures, revealed as a peak in the magnetic susceptibility for some of these samples at the Néel temperature T_N, as shown in Fig. 4 and listed in Table I. Data for R=Gd, Tb, and Dy represent χ_{dc} from static (dc) magnetization measurements taken in a field of 10 Oe (100 Oe for R=Gd) after zero-field cooling (ZFC) and during field cooling (FC). Data for R=Ho and Er are from low-temperature ac magnetic-susceptibility χ_{ac} measurements.

Two interesting aspects of the magnetic-susceptibility data are (1) there is only a small decrease in $\chi(T)$ below T_N as $T \to 0$ [the ratio $\chi(0)/\chi(T_N)$ is much larger than the theoretical value of 2/3 for an isotropic, uniaxial AFM powder specimen[7]] and (2) irreversibility in χ_{dc} appears below an onset temperature T_{irr}, reminiscent of spin-glass freezing. The large $\chi(0)/\chi(T_N)$ ratio is characteristic of spin glasses, but can also occur for an antiferromagnetically ordered fcc lattice due to low anisotropy energy.[8] In the latter case, the measured susceptibility below T_N approaches $\chi_\perp$ (in which the antiparallel moments are perpendicular to the applied magnetic field H), which is more energetically favorable than $\chi_\parallel$ (moments parallel to H). Paramagnetic impurities could also increase the measured value of $\chi(0)/\chi(T_N)$. The irreversible $\chi_{\mathrm{dc}}(T)$ for $\mathrm{GdPd}_2\mathrm{Pb}$ was measured with H=1, 10, 100, and 200 Oe, with little change in $\chi(T)$ or T_N. This observation, as well as the observed scaling of T_N with the de Gennes factor (described below), and the electrical-resistivity results (described above) eliminate the possibility that these anomalies are due to superconductivity. The irreversibility in the magnetization might be due to structural disorder (defects) in the samples, which could give rise to

TABLE I. Physical parameters for $M\mathrm{Pd}_2\mathrm{Pb}$. A dash indicates that the entry is not applicable to nonmagnetic M ions. * indicates not detected above 0.1 K.

M	a (Å)	μ_{eff} (μ_B)	θ_{CW} (K)	T_c (K)[a]	T_N (K)
Sc	6.63	0	–	2.4	–
Y	6.74	0	–	2.3	–
Gd	6.81	8.51	−17.3	*	4.5
Tb	6.79	10.17	−16.9	*	2.8
Dy	6.76	11.13	−9.8	*	2.4
Ho	6.75	11.10	−6.5	*	0.8
Er	6.76	9.77	−5.2	*	0.6
Tm	6.72	7.85	−2.7	2.1	*
Yb	6.73	4.15	−3.6	2.8	*
Lu	6.73	0	–	2.4	–
Th	6.88	0	–	*	–
U	6.85	2.8	−51	*	35

[a]Onset temperature of superconducting diamagnetic transition in static magnetic susceptibility.

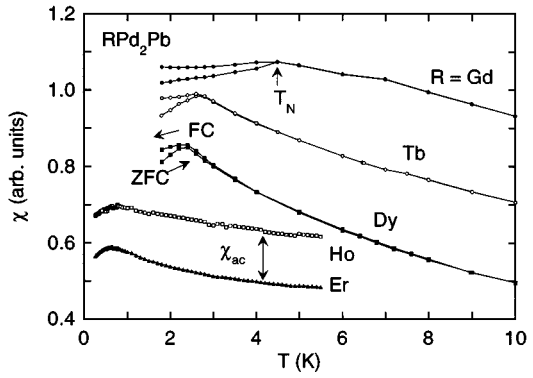

FIG. 4. Low-temperature magnetic susceptibility χ vs temperature T of $R\mathrm{Pd}_2\mathrm{Pb}$ single crystals, revealing antiferromagnetic order below the Néel temperature T_N, determined from the cusp in the data. The data for R=Gd, Tb, and Dy are from dc measurements taken in fields of 100, 10, and 10 Oe, respectively, upon zero-field cooling (ZFC) and field cooling (FC). The data for R=Ho and Er are from ac susceptibility measurements as described in the text.

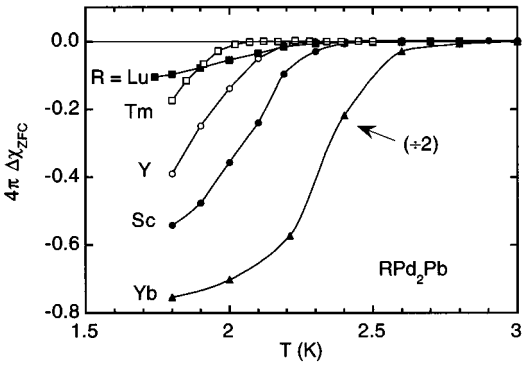

FIG. 5. Superconducting contribution to the magnetic susceptibility $\Delta\chi$, after zero-field cooling (ZFC) and then applying a 10 Oe field, for single-crystal specimens of the $R\mathrm{Pd}_2\mathrm{Pb}$ compounds which were found to be superconducting. The data for $R=$Tm and Yb were corrected for the magnetic background contribution of the R ions.

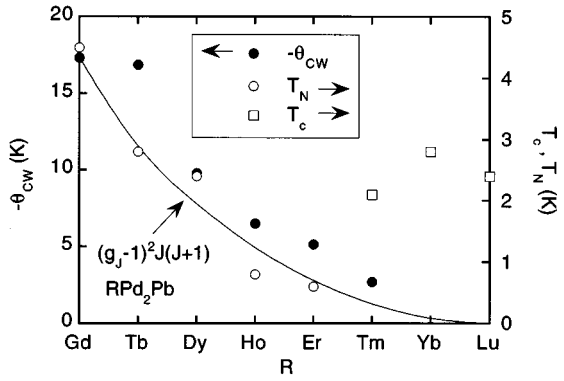

FIG. 6. Curie-Weiss temperatures θ_{CW} (solid circles), Néel temperatures T_N (open circles), and onset superconducting critical temperatures T_c (open squares) of the $R\mathrm{Pd}_2\mathrm{Pb}$ compounds, derived from magnetic-susceptibility measurements. The values θ_{CW} and T_N are compared to the de Gennes factor $(g_J-1)^2J(J+1)$, represented by the solid line, and normalized to the values for $R=$Gd.

spin-glass-like behavior, or possibly geometrical frustration of the ordered moments on the fcc lattice.

The existence of bulk superconductivity was confirmed for some of the $R\mathrm{Pd}_2\mathrm{Pb}$ samples from dc magnetic-susceptibility measurements, taken upon both ZFC and FC in a magnetic field $H=10$ Oe. ZFC data are shown in Fig. 5. The $\chi(T)$ data were irreversible with the FC data being typically 50% of the ZFC values for each sample, which we attribute to flux pinning. A significant diamagnetic response, indicative of bulk superconductivity, is observed for $R\mathrm{Pd}_2\mathrm{Pb}$ compounds in which R is a nonmagnetic trivalent ion, including $R=$Sc, Y, and Lu. Evidently, superconductivity is the ground state of this system in the absence of magnetic pair breaking by magnetic R ions. The d electrons of the Pd ions are believed to be mainly responsible for superconductivity in these compounds.[1] Curiously, superconductivity was not observed down to 1.8 K for $\mathrm{ThPd}_2\mathrm{Pb}$, Th being a nonmagnetic tetravalent ion. Superconductivity was also observed for $R=$Tm and Yb, which are trivalent magnetic ions with the smallest values of the de Gennes factor $(g-1)^2J(J+1)$ among the heavy magnetic rare earths. The $\Delta\chi$ data shown in Fig. 5 for $R=$Tm and Yb were obtained by subtracting the magnetic contribution of the Tm and Yb ions, respectively. As shown in Fig. 5, the diamagnetic shielding fractions, estimated from the ZFC measurements, vary from $\sim$10% to $\sim$60% for single-crystal specimens, and are as high as 140% for polycrystalline $\mathrm{YbPd}_2\mathrm{Pb}$. These values should be multiplied by a factor of $\sim$2/3 to account for the demagnetization correction if one approximates the cube-shaped crystals as spheres.

The superconducting transitions are rather broad, with onset temperatures ranging from 2.1 to 2.8 K (see Table I). Previous measurements of T_c for arc-melted polycrystalline samples of $\mathrm{YPd}_2\mathrm{Pb}$ yielded higher values of $T_c=4.76$ (Ref. 1) and 4.05 K.[9] The precise value of T_c is known to be highly sensitive to the stoichiometry in these Heusler systems, with a possible correlation with lattice parameter, which could be due to a sharp feature in the electronic density of states.[1] It is not clear what value of T_c represents that of the stoichiometric compound $\mathrm{YPd}_2\mathrm{Pb}$. We note, however, that one must be very careful to account for the effects of any superconducting impurities including Pb ($T_c=7.2$ K) and $\mathrm{Pb}_2\mathrm{Pd}$ ($T_c=3.0$ K).

Magnetic interactions in a metal with rare-earth ions are governed by the sf exchange interaction between the conduction electron spins **s** and the total angular momentum **J** of the local $4f$ states, given by the Hamiltonian $\mathscr{H}_{sf}=-2\mathscr{J}_{sf}(g_J-1)\mathbf{J}\cdot\mathbf{s}$, where $\mathscr{J}_{sf}$ is the exchange coupling parameter and g_J is the Landé g factor of the rare-earth ion. The factor (g_J-1) results from replacing the total spin **S** with its projection onto the total **J** for rare earths with finite orbital angular momentum **L**. For superconducting metals, this interaction leads to magnetic pair breaking as described, for example, by the Abrikosov-Gorkov theory. For a lattice of rare-earth ions, this interaction leads to the RKKY indirect exchange interaction between rare-earth ions, with Hamiltonian $\mathscr{H}_{\mathrm{RKKY}}=-\Sigma\mathscr{J}_{\mathrm{eff}}\mathbf{J}_i\cdot\mathbf{J}_j$, where $\mathscr{J}_{\mathrm{eff}}\sim\mathscr{J}_{sf}^2(g_J-1)^2$. The RKKY interactions are responsible for magnetic order at low temperatures and magnetic correlations at high temperatures which result in finite Curie-Weiss temperatures. If the magnitude of $\mathscr{J}_{sf}$ is constant, the characteristic temperatures T_N and θ_{CW} are predicted to scale among the rare earths with the de Gennes factor $(g_J-1)^2J(J+1)$, which represents the square of the component of the total spin **S** in the total **J** direction, $|(\mathbf{S}\cdot\mathbf{J})\mathbf{J}|^2$.

Figure 6 summarizes the results of the magnetic-susceptibility measurements on the $R\mathrm{Pd}_2\mathrm{Pb}$ compounds, showing θ_{CW}, T_N, and T_c for the heavy rare-earth R ions. Both θ_{CW} and T_N scale approximately with the de Gennes factor $(g_J-1)^2J(J+1)$, represented by the solid line in Fig. 6 (normalized to the values for $R=$Gd). Crystalline electric field effects could be responsible for deviations from this scaling. It is interesting to note that the values of T_N and θ_{CW} are very small compared to other rare-earth intermetallic compounds, implying small exchange interactions. Of particular interest is the existence of superconductivity for $R=$Tm and Yb. Apparently, because of the small de Gennes factors, the magnetic pair breaking due to the magnetic Tm and Yb ions is not sufficiently strong to destroy superconductivity. In addition, since Tm is a non-Kramer's ion, it is possible for it to have a nonmagnetic CEF ground state, which might also reduce magnetic pair breaking. Supercon-

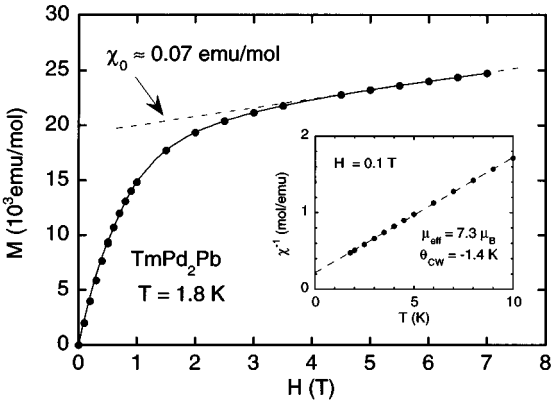

FIG. 7. Isothermal magnetization M vs magnetic field H of $TmPd_2Pb$ single crystals at $T=1.8$ K. The solid line is a guide to the eye. The dashed line represents a linear fit to the high-field data with the slope $\chi_0=0.07$ emu/mol. Inset: Low-field ($H=0.1$ T) inverse magnetic susceptibility χ^{-1} vs temperature below 10 K. The dashed line represents a fit of the data to a Curie-Weiss law for $1.8\leqslant T\leqslant 10$ K with $\mu_{\rm eff}=7.3\mu_B$ and $\theta_{\rm CW}=-1.4$ K, revealing magnetic behavior of the Tm ions.

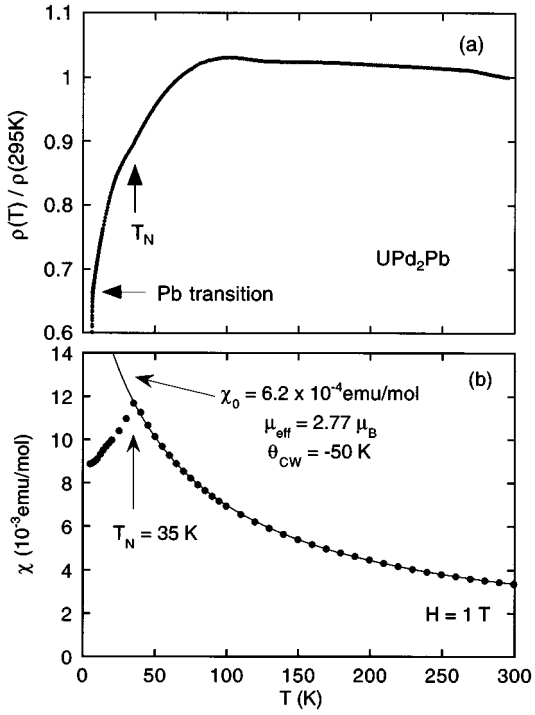

FIG. 8. Temperature T dependence of (a) the normalized electrical resistivity $\rho(T)/\rho(295\ \mathrm{K})$ and (b) the dc magnetic susceptibility $\chi(T)$ of UPd_2Pb (polycrystalline sample), revealing antiferromagnetic order of the U ions below $T_N=35$ K.

ductivity was previously observed in $TmPd_2Sn$ and $YbPd_2Sn$ with T_c values of 2.8 and 2 K, respectively,[1,3] and $YbPd_2Sn$ was discovered to exhibit coexistence of superconductivity and antiferromagnetic order of the Yb ions below $T_N=0.23$ K.[3] This coexistence has been attributed to the small de Gennes factor of Yb. The $TmPd_2Sn$ compound was postulated to have a nonmagnetic CEF ground state. There does not appear to be any sign of magnetic order for $TmPd_2Pb$ or $YbPd_2Pb$ down to 1.8 K from our magnetic-susceptibility measurements.

From magnetic-susceptibility and ^{119}Sn Mössbauer measurements on $TmPd_2Sn$, Malik, Umarji, and Shenoy[10] deduced that the Tm^{3+} ions have a Γ_3 nonmagnetic ground state with a first excited triplet state $\sim$1 meV ($\sim$10 K) above the ground state. Shown in Fig. 7 are magnetization $M(H)$ data for $TmPd_2Pb$ crystals at 1.8 K, measured in fields H up to 7 T. The $M(H)$ data are nonlinear and consist of a contribution that appears to saturate like a Brillouin function in high fields and a linear term with a slope $\chi_0=0.07$ emu/mol, represented by the dashed line. The linear term could be a second-order van Vleck susceptibility term. Extrapolation of the linear term to zero yields the saturation magnetization of $\sim 19\times 10^3$ emu/mol, corresponding to $g_J J=3.4\mu_B$, which is less than the saturation moment of $7\mu_B$ for the full Tm^{3+} multiplet. This reduced value could be due to the cubic CEF which splits the multiplet such that the $\Gamma_5^{(2)}$ triplet, which has the magnetic moment $g_J\langle\Gamma_5^{(2)}|J_z|\Gamma_5^{(2)}\rangle=3.13\mu_B$, lies lowest.[11] A nonmagnetic ground state appears to be ruled out unless the CEF splittings are very small compared to 1.8 K.

Shown in the inset is a plot of the temperature dependence of the inverse magnetic susceptibility from 1.8 to 10 K as measured in a low field of 1 kOe where $M(H)$ is approximately linear down to 1.8 K. The dashed line in the inset represents a fit to a Curie-Weiss law in this temperature range, which has nearly the same $\mu_{\rm eff}$ and $\theta_{\rm CW}$ as the high-temperature fits, again suggesting that the CEF splitting is very small, or that the $\Gamma_5^{(2)}$ triplet lies lowest in energy. In either case, it is surprising that superconductivity exists in $TmPd_2Pb$ despite the highly magnetic character of the Tm ions even at low temperatures $T\sim T_c$.

UPd_2Pb

In a previous study of uranium-based ternary compounds with the chemical formula UT_2X with T=Pd, Au and X=In, Si, Ge, Sn, Sb, it was found that only those with M=In formed the cubic Heusler structure.[4] The others revealed a more complicated structure in the x-ray-diffraction patterns, believed to be orthorhombic. None of those materials studied were superconducting down to 80 mK. The compound UPd_2Sn, however, displayed characteristics of valence fluctuation or Kondo lattice phenomena below a characteristic temperature $\sim$10 K, and is considered[4] to be a nonmagnetic, nonsuperconducting heavy-electron material. In particular, the electronic specific-heat coefficient $\gamma=C_{\rm el}/T$ was found to be strongly temperature dependent with a maximum value of $\sim$270 mJ/mol K^2 at 9.7 K and an extrapolated value of $\sim$70 mJ/mol K^2 at $T=0$ K.

We have synthesized polycrystalline samples of UPd_2Pb and found that it forms the cubic $L2_1$ Heusler structure. The cubic lattice parameter $a=6.85\pm0.01$ Å is the largest of all the MPd_2X $L2_1$ Heusler compounds (see Table I), except perhaps for a mixed-phase $ThPd_2Pb$ sample which had a comparable value $a=6.88\pm0.05$ Å. It is interesting that this compound forms while MPd_2Pb compounds with M=Sm and Eu, which would have smaller or comparable lattice parameters, do not. It is possible that the hybridization of the $5f$ electrons with the conduction-band states stabilizes this

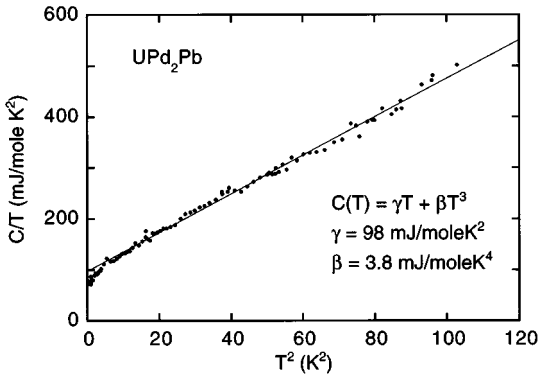

FIG. 9. Low-temperature specific heat C, plotted as C/T vs T^2, for UPd_2Pb. The solid line represents a linear fit of the relation $C/T=\gamma+\beta T^2$, as described in the text. The large value of the Sommerfeld constant γ is suggestive of heavy-fermion behavior.

crystal structure. We subsequently measured $\rho(T)$, $\chi(T)$, and $C(T)$ in order to characterize it for possible heavy-fermion behavior.

The temperature dependences of the normalized electrical resistivity and magnetic susceptibility of UPd_2Pb are shown in Figs. 8(a) and 8(b), respectively. The electrical resistivity $\rho(T)$ increases by only a few percent with decreasing temperature down to ~100 K, below which $\rho(T)$ decreases. The negative temperature coefficient of resistance above 100 K is indicative of Kondo-like magnetic scattering and is a typical feature of heavy-fermion materials, as is the subsequent drop below 100 K. A small kink in the $\rho(T)$ data is observed at $T=35$ K, which we attribute to antiferromagnetic ordering of the U ions, inferred from the magnetic-susceptibility data in Fig. 8(b). Like the other MPd_2Pb polycrystalline samples, $\rho(T)$ drops suddenly below 7.2 K due to Pb inclusions. The low-temperature resistivity of MPd_2Pb could be studied by applying a magnetic field sufficient to destroy the superconductivity of Pb and Pb_2Pd impurity phases.

The magnetic susceptibility of UPd_2Pb is shown in Fig. 8(b). A sharp cusp is observed at $T=35$ K, which we attribute to AFM order of the U ions. In contrast to the RPd_2Pb compounds which exhibit AFM order, the ratio $\chi(0)/\chi(T_N)\approx 0.75$ for UPd_2Pb, which is only slightly larger than the theoretical value of 2/3 for an isotropic, uniaxial AFM powder specimen.[7] At higher temperatures, the $\chi(T)$ data can be described by a Curie-Weiss law plus a constant χ_0, $\chi(T)=N\mu_{\rm eff}^2/3k_B(T-\theta_{\rm CW})+\chi_0$, represented by the solid line, with $\mu_{\rm eff}=2.77\mu_B$, $\theta_{\rm CW}=-50$ K, and $\chi_0=6.2\times10^{-4}$ emu/mol. The value of the effective moment is somewhat smaller than the free-ion values for trivalent ($3.62\mu_B$) and tetravalent ($3.58\mu_B$) U ions. The paramagnetic constant χ_0 could be due to an enhanced Pauli susceptibility for a heavy-fermion compound. Significant CEF splitting ($\Delta_{\rm CEF}\sim100$ K) might also give rise to the observed deviation from free-ion behavior. Not shown in Fig. 8(b), the $\chi(T)$ data reveal slightly irreversible behavior at temperatures below T_N.

Shown in Fig. 9 are low-temperature specific-heat data for UPd_2Pb, plotted as C/T vs T^2, for $0.5\leqslant T\leqslant 10$ K. The solid line represents a least-squares fit of the data to the equation $C(T)=\gamma T+\beta T^3$, with $\gamma=98$ mJ/mol K^2 and $\beta=3.8$ mJ/mol K^4. The value of the Sommerfeld coefficient γ is at least an order of magnitude larger than that of a normal metal, although it is small compared to prototypical heavy-fermion compounds for which $0.25\lesssim\gamma\lesssim1$ J/mol K^2.[12] However, the U ions are antiferromagnetically ordered at these temperatures, which might be responsible for the observed values of the coefficients γ and β. Measurements of $C(T)$ to higher temperatures will give information about the ordering, as well as a measure of γ above T_N.

CONCLUSION

Single crystals of RPd_2Pb with very small amounts of impurity phases were fabricated. Measurements of magnetic susceptibility revealed bulk superconductivity for $R=$Sc, Y, Tm, Yb, and Lu, with $T_c\approx2$–3 K. These values are lower than expected; a T_c value as high as 4.76 K was previously reported for YPd_2Pb. The discrepancy is most likely due to differences in sample composition and/or quality. In particular, the T_c's of these Heusler compounds are known to be sensitive to exact stoichiometry; off-stoichiometric polycrystalline samples might yield higher T_c values. The magnetic rare-earth ions order antiferromagnetically with very low Néel temperatures $T_N\leqslant4.5$ K. Both T_N and $\theta_{\rm CW}$ scale approximately with the de Gennes factor. It is unlikely that the Tm ions in $TmPd_2Pb$ have a nonmagnetic ground state, making it more surprising that it is superconducting. $ThPd_2Pb$ was not superconducting above 1.8 K. The Heusler compound UPd_2Pb orders antiferromagnetically below 35 K, and displays many characteristics of a low effective mass heavy-fermion material.

ACKNOWLEDGMENTS

This research was supported by NSF Grant No. DMR 91-07698. J.H. acknowledges support from DAAD. Some of the equipment used in this research was part of the UCSD Center for Interface and Materials Sciences, provided by a grant from the Keck Foundation.

*Present address: Energy Science Laboratories, 6888 Nancy Ridge Dr., San Diego, CA 92121-2232.

†Present address: National High Magnetic Field Laboratory, 1800 East Paul Dirac Dr., Tallahassee, FL 32306-4005.

[1] M. Ishikawa, J.-L. Jorda, and A. Junod, in *Superconductivity in d- and f-Band Metals*, edited by W. Buckel and W. Weber (Kernforschungszentrum, Karlsruhe, 1982).

[2] J. H. Wernick, G. W. Hull, T. H. Geballe, J. E. Bernardini, and J. V. Waszczak, Mater. Lett. **2**, 90 (1983).

[3] H. A. Kierstead, B. D. Dunlap, S. K. Malik, A. M. Umarji, and G. K. Shenoy, Phys. Rev. B **32**, 135 (1985).

[4] C. Rossel, M. S. Torikachvili, J. W. Chen, and M. B. Maple, Solid State Commun. **60**, 563 (1986).

[5] A. M. Umarji, S. K. Malik, and G. K. Shenoy, Solid State Commun. **53**, 1029 (1985).

[6] B. W. Roberts, J. Phys. Chem. Ref. Data **5**, 581 (1976).

[7] J. H. Van Vleck, J. Chem. Phys. **9**, 85 (1941); T. Nagamiya, Prog. Theor. Phys. **6**, 342 (1951).

[8] J. H. Van Vleck, J. Phys. Radium **12**, 262 (1951).
[9] M. J. Johnson and R. N. Shelton, Solid State Commun. **52**, 839 (1984).
[10] S. K. Malik, A. M. Umarji, and G. K. Shenoy, Phys. Rev. B **31**, 6971 (1985).
[11] K. R. Lea, M. J. M. Leask, and W. P. Wolf, J. Phys. Chem. Solids **23**, 1381 (1962).
[12] Z. Fisk, D. W. Hess, C. J. Pethick, D. Pines, J. L. Smith, J. D. Thompson, and J. O. Willis, Science **239**, 33 (1988).